

**Linac-Driven Plutonium Breeder
Target-Blanket Physical Parameters**

**I.Kh. Ganev, A.V. Lopatkin, L.V. Tocheniy
RDIPE, Moscow**

LINAC- driven Plutonium Breeder

Target-Blanket Physical Parameters

I. Kh. Ganev, A. V. Lopatkin, L. V. Tochjenyj

I. Introduction

Progress achieved in recent years by science and technology in accelerator facilities has stimulated interest to the concept of electrofusion reactor (EFR) - the facility that is capable to supply power, secondary nuclear fuel, as well as burn-out radioactive wastes (RAW) (1). This interest is conditioned by such fundamental features of electronuclear method as:

- nuclear safety (subcriticality);
- high fuel production rate;
- possibility to generate neutron and charge particle fluxes in a broader energy range (including threshold reactions) compared to the one used in fission and fusion-type reactors (2,3).

The present. paper discusses physical aspects of the approach and preliminary study of EFR blanket-target carried out at RDIPE (Research and Development Institute of Power Engineering) within the framework of the concept analysis of the EFR fuel production method. It is evident that problem of blanket-target as an energy production facility and blanket-target as a RAW, burning out facility have much in common both in physical/engineering and computational/methodological aspects.

EFR includes:

*RDIPE-NIKIET
(Moscow, Russia)*

- charged particle accelerator within energy range from hundreds of MeV up to several GeV;
- target where neutrons are generated by the deep splitting reactions cascade;
- blanket where neutrons can be used for producing power and useful nuclides or for RAW burning out;
- radiation protection.

Linear accelerator (LA) operating in continuous mode is considered as a base one. There is substantial scientific and research basis for developing and building LA with the beam power order of hundreds of MWt and with the efficiency no less than 50 %. Protons, deuterons, α -particles, as well as more heavy nuclei can be used in EFR as accelerating particles. Neutron yield is proportional to the kinetic energy of an incident particle at the moment of the first inelastic collision with the target substance nucleus. Therefore, maximum neutron yield per consumed power unity is achieved at that time when the fraction of particle initial power consumed for the environment ionization prior to the first collision is minimal. Kinetic energy fraction spent on ionization is determined as follows:

$$\Delta E = - \frac{1}{E_0} \int_0^{\lambda_{in}} e^{-x/\lambda_{in}} \frac{\partial E}{\partial x} dx$$

where E_0 - the energy of the incident particle, λ_{in} - free path prior to inelastic collision [2].

Ionization losses are less than 10 % for the energy range

exceeding 3 GeV, the lowest being-for deuterons and protons. As the calculations show (4), in the large natural Uranium target proton (1GeV) gives neutron yield only by 10 % lower, than deuteron under more favorable radiation conditions. This is the principal cause why the linear accelerator has been chosen: proton beam, energy - 1GeV, current - 0.3 A.

EFR blanket-target complex is considered here as the dual-purpose object, i.e. producer of the secondary fuel and supplier of the thermal power.

Computation methods for neutron fields and power density, breeding, isotopic composition of irradiated fuel calculations have been developed to justify physical and technical solutions.

2. Software and methodical ensuring

2.1. ИПОРАБ code for neutron field computation

According to nuclear transmutations, energy and types of particles participating in all the variety of the processes that occur in the substance being penetrated by high-energy particles can be subdivided into two stages: in- and internucleus cascades and low-energy particles diffusion. At the first stage we consider transfer of adrons with energy range from 10-20 MeV to several GeV and forming low-energy particle spatial-energy distribution. At the second stage we consider in detail their transfer within the energy range lower than 10-20 MeV.

For the first stage the following codes are mostly well-known (Monte-Carlo method): KACKAD (Cascade) (J ITNR),

MARS (IHEPh), NNTC, HETC (Oak-Ridge NL), SITHA (RI named after Khlopina), SVTWR (Institute of Nuclear power of the Belorussian Academy of Sciences).

At RDIPE a quick-operating method is implemented in IPO-PAB code. At the first (high-energy) stage initial neutron spatial-energy distribution is determined by means of approximal dependence that are based on benchmark calculations and experiments. At the second (low energy) stage under preset initial neutron distribution a quick-operating method of two-dimensional (R-Z or X-Y) multigroup calculations of neutron fields and functional is used. Fuel isotopic composition changes under irradiation and simulation of regional refuellings are envisaged by calculations. 28-group (14-0 MeV) cross section are ensured by APAMAKO code. Neutron transport (with external source) equation is solved by means of partial-permanent approximation (at temporary step).

Quasi stationary equation is solved by means of neutron flux density resolution according to subsequently generated neutron generations:

$$\phi(\vec{r}, E) = \sum_{n=1}^{\infty} \phi_n(\vec{r}, E)$$

$\phi_1(\vec{r}, E)$

where ϕ_1 - field generated by source neutrons, with $n \geq 2$ is determined by the solution of transport equation with fission source generated by the previous neutron generations. In multigroup diffuse-transport approximate on the neutron transport equation is solved by means of iteration synthesis,

arbitrary spatial variable distribution and energy group convolution in XY and RZ geometry.

Approximation to an infinite number of generations is conducted in the following way. Multiplication factor K is determined for each generation. It can be stated that if K relative change is less than preset accuracy

$$\left| \frac{K_{ef}^n - K_{ef}^{n-1}}{K_{ef}^n} \right| \leq \delta$$

neutron flux density spatial distribution from generation to generation remains similar and differs in amplitude.

In this case we have the following equation.

$$\Phi(\bar{z}, E) = \sum_{n=1}^{\infty} \Phi_n(\bar{z}, E) \approx \sum_{n=1}^{N-1} \Phi_n(\bar{z}, E) + \frac{\Phi_N(\bar{z}, E)}{1 - K_{ef}^N}$$

Electronuclear neutron data - namely, energy spectra, multiplicity, spatial distribution - have been gained by means of specific codes based on Monte-Carlo method (Fig. 1,2). In nuclei mixture multiplicity is determined by the following relationship:

$$N_{\Sigma} = \frac{\sum_{i=1}^I \eta_i \sigma_{in}^i S_i}{\sum_{i=1}^I \sigma_{in}^i S_i}$$

where ρ_i i -type nucleus concentration,

$\sigma_{in}^i = 38.5 A_i^{5/4}$ (mbn) - cross section of inelastic high energy particles interaction with A_i mass nucleus.

Disagreement between ИПОРАБ Uranium target test calculations and data obtained by means of specific codes does not exceed 8 % in integral rates calculations of fission and capture reactions for the proton beam of 1 GeV and 1 % in case of Cf-252 fission neutron source.

2.2. BLC code for calculating nuclide composition kinetics, value function and sensitivity.

BLC code /5/ is implemented in order to solve the following type of equations of nuclide composition changes

$$\frac{d\vec{x}}{dt} = \hat{A} \vec{x}$$

$$\vec{x}(t_0) = \vec{x}_0$$

where \vec{x} -nuclide concentration vector (\vec{x}_0 - initial conditions),

\hat{A} - matrix, its components are parameters of nuclides generation and burning out. Runge-Kutt method is used for integrating. BLC code is provided by the library of nuclear data for different reactor type, including EFR, as well as codes-processors of BLC connecting to the program of neutron spectra computation and cross-section averaging. The following nuclear reactions are taken into account, namely: fission, radiation capture, n-, λn -type reactions with $n=2..7$. In EFR target up to 15 % of neutrons can have energy within the range of 10.5-100 Mev. Method of small perturbations is used for estimating sensitivity to uncertainties of initial data (nuclear data, initial conditions, neutron flux):

$$\frac{\delta X_i^k}{X_i^k} = S_{ijk} \frac{\delta \lambda_{jk}}{\lambda_{jk}}$$

where S_{ijk} - "i" nuclide sensitivity coefficient to parameter version of "K" process on "j" nuclide (λ_{jk} - decay constant, G_{kj} - cross section)

$$S_{ijk} = -\frac{1}{X_i} \int_{\Delta t} \lambda_{kj} (X_j X_i^* - X_j X_j^*) dt$$

* solution of the task conjugated with the initial one (ajoint)

3. Investigation of possible EFR blanket neutron-physical parameters

3.1. Production of secondary fissile fuel

Table I presents data for the idealized blanket, without structural materials.

The spot where proton beam hits is deepened into the target to minimize the reflection effect. Plutonium production is. by 10-50 % lower in uranium silicides, carbides, nitrides, oxides than in uranium metal.

Table 1

Process rates in the target of infinite reactors

Mater i al	N_{γ}	νN_f	λ_+	N_c	Pu kg/year	W , MW
Umet	56.8	0.787	0.278	1.541	2039	1248
UO	44.7	0.586	0.208	1.400	1440	857
UC	51.1	0.638	0.226	1.436	1705	992
U C	48.6	0.598	0.212	1.407	1588	918
UC	46.4	0.566	0.202	1.371	1488	862
UN	50.5	0.607	0.215	1.415	1543	950
U Si	53.2	0.712	0.252	1.487	1830	1105
US i	47.3	0.607	0.216	1.412	1525	913
US i	40.7	0.503	0.180	1.339	1278	740

US i	35.8	0.434	0.156	1.291	1021	635
------	------	-------	-------	-------	------	-----

Three groups of blanket versions are considered. The first two are related to the decisions drawn on the basis of modern sodium and water-cooled reactors, the third one - to versions based on uranium melts (ultimate estimates).

Three versions of the first group (I-A compact U-containing target, I-B - jet-type lead target, I-C - blanket direct irradiation by protons) are based on an integral layout of the BH-600 type reactor. Proton beam is introduced vertically (I-A, I-B) or horizontally (I-C).

Dependence of main parameters on uranium/steel/sodium-to-fuel composition relation is investigated. The following aspects are also investigated: parameters temporal changes under irradiation, plutonium build up, its nuclide composition, quantity of fission products, parameter values obtained under selected thermal loads restrictions. The possibility to increase thermal power and redundant plutonium production rate is shown in Fig. 3-5.

Peculiarities of the blanket with hard neutrons spectrum neutron spectrum similar to that of fast reactor;

- high neutron yield in uranium-plutonium fission reactions;
- high production of redundant plutonium;
- high probability of U-239 fission;
- high plutonium equilibrium concentration in fuel.

Blankets with degraded spectrum (II-A, II-B versions) are

considered. By shifting neutron spectrum into resonance and thermal region neutron fission yield decreases, neutron balance deteriorates, plutonium equilibrium concentration in fuel decreases. Parameters are rather sensitive to volumetric proportion of water in the fuel channel with water/fuel ratio less than 1/4. In P-A version neutrons are generated in a narrow surface layer, i.e. fuel assemblies of the first row. In version II-B due to variations of U-content in fuel elements zone of neutron generation and high power density is deepened into the target. The results are: a more compact blanket-target system, neutron yield is less by 12 %, leakage is higher (Fig. 6-7).

EFR ultimate capabilities are shown by way of example of blanket versions with uranium melt or uranium-bismuth (U-Bi), where participation of structural materials in intensive nuclear reactions is excluded, a better neutron balance is achieved, continuous refueling is possible (Fig. 8). Possible heat-removal schemes can be suggested:

- through vessel walls;
- metal vapours bubbling (for example-sodium) through melt;
- cooling melt surface;
- uranium vapour removal into contact heat exchanger.

It is possible to lower temperature of the circulating material in case of U-Bi alloy.

3.2. Spatial peaking

The main method for levelling electronuclear neutrons generation density and power density within the target volume is to change the average substance density through target cross-section (average macrosection of interaction) towards the directions of proton movement. This can be achieved by changing:

- jet density in the target;
- jet diameter;
- fuel assembly pitch;
- cross-section area of proton beam interaction zone (funnels, inclined planes, etc.). "

Within the energy range more than 80 MeV microsection of nucleon-nucleus interaction is energy weakly dependant. Neutron generation is on the whole determined by inelastic interactions:

$$q_n(z) = a \Sigma(z) \Phi_0 \exp\left(-\int_0^z \Sigma(x) dx\right)$$

For $q_n(z) = \text{const}$ the following must be true:

$$\Sigma(z) = \frac{\Sigma_0}{1 - z \Sigma_0} \quad 0 \leq z \leq \frac{1}{\Sigma_0} - \frac{1}{\Sigma_{max}}$$

"Z" reading is deepen into the target by value $\Delta Z = 0.5z$, where growth of $q(z)$ is observed. $q(z) = \text{const}$ is possible on a

limited region that is determined by Σ_0 and Σ_{max} of the target's macrosections (where Σ_0 is inlet macrosection and E_{max} - maximum possible macrosection) (Fig. 9-11).

3.3. Nuclide composition

In EFR conditions of plutonium production substantially differs from that of traditional one (as in fast reactors) by means of neutron spectrum formed in blanket, because in EFR these conditions are determined by the effect and participation of source (target) high-energy neutrons. For example, in a large target of depleted uranium a fraction of neutrons with energy from 10.5 up to 100 MeV, generated by 1 GeV proton (without taking into account fissions in the reactor energy range) constitutes about 20 %. When fissions are taken into account this fraction decreases to 5-5 %, but still remains significantly higher than in fission reactors (0.2 %). In the energy range above 15 MeV the main nuclear reactions initiated by neutrons are fission and n, xn-type reactions where $x=1-7$. Charged particles yield is by 3 and more orders lower than in neutron channel. Energy dependence of neutron interaction sections with energy up to 70 MeV for U-238, U-234, U-235, Pu-239 nuclei are calculated on the assumption that the process of eliminating nuclear excitation upon neutron capture consists of a series of sequential stages accompanied by emission of neutrons, protons, alpha-particles, - (gamma) -quanta and fission. Table 2 shows channel cross-sections of particle emission at each stage. The

preferable channel is neutron emission (,2.5 barns with full cross-section of 3 barns) i.e. U-238 is mainly produced. The probability of charged particles emission is by 4-5 order lower. Then U-238 nucleus decays (2nd stage of decay). At first five stages the preferable channels are neutron channel and fission. The newly formed U-235 nucleus has maximum excitation energy of 8.1 MeV, which is almost by 3 MeV more than the neutron binding energy. However, due to angular moment. limitations radiation channel plays the basic role, excitation is eliminated by gamma-quantum emission, U-235 residual nucleus transforms into ground state.

Table 2

Channel cross-sections of the yield of neutrons, protons, gamma-quanta, alfa-particles and U-238(n, Xn) fission reaction at each stage of decay (millibar), E=28 MeV.

Decay channel								
	n		p		a		(n, f)	
1	2.47	+3	1.35	-2	1.94	-1	5.69 -1	5.15 +2
2	1.99	+3	1.95	-3	2.40	-1	2.09 -1	4.84 +2
3	1.49	+3	1.35	-5	4.50	-1	3.71 -2	4.98 +2
4	8.69	+2	1.45	-7	2.48	+1	1.28 -3	6.11 +2
5	2.94				7.38	+2	1.15 -8	1.28 +2

From Fig.12 it is seen that there are regions of neutron energy where one of n, Xn -type reactions predominantly proceeds. For example, on U-238 nucleus within the 23-32 MeV range proceeds the following reaction: $U-238(n, 4n)$, 40-50 MeV- $U-238(n, 6n) U-233$.

Cross-sections of threshold (n, Xn) reactions have the shape of bell-like curves that strongly increase near the threshold, with its maximum near the threshold of the next reaction and with its width increasing with the number of emitted particles. Maximum cross-section value also changes with energy in accordance with the fact that full probability of the decay in other channels (mainly, ~~long-term~~ ^{fission}) increases with the number of emitted particles.

In EFR blanket neutrons of energy above 15 MeV, and n, Xn -type reactions substantially change proportions of U-isotope formation rates. Light U-isotopes, as well as Pu-isotopes are accumulated in much larger quantities than in fission reactors. Fuel isotopic composition depends on blanket composition, on neutron spectrum being formed in the blanket.

Calculations are made to meet the condition of Pu accumulation in fuel up to 1 % and 5-6 % under continuous refueling mode.

Versions of typical neutron spectra are considered:

- a) metallic uranium (without structural materials and coolant);
- b) fuel assembly (FA) of the fast reactor, metallic uranium - I-C version;
- c) metallic uranium with water coolant - P-A version.

Direct irradiation by target protons is assumed.

Isotopes from Th-228 to Cm-246 are considered in nuclide intertransmutation scheme. The following matters are taken into account: decay (BLC code), neutron reactions such as (n), (n, f), (n, Xn), with (n,2n) for all nuclides; (n,3n)- for U and Pu; (n, 4n) - for U-238 and Pu-239; (n, Xn) - with $X=5$ - for U-238. n, Xn reaction cross-sections are calculated by Yu. N. Shubin /5/. Total flux density is assumed to be constant - 510 n/(cm² s). Initial U-composition - 0.3 % U-235; 99.7 % U-238, Isotopic composition of uranium and plutonium is shown in tab. Light isotopes of uranium (including U-235) and plutonium are accumulated under irradiation. U-232 content in uranium is approximately by 1000 times higher than in the fast reactor blanket. U-232 equilibrium content in uranium (1-10 %) conforms with the case of Fission reactor with - uranium-thorium fuel cycle (Fig. 14-16).

U-232 accumulation sensitivity analysis has shown the maximum "value" of the reaction channel U-238 (n,7n) U-232, exceeding others by 2 orders, as well as importance of neutron absorbing reaction by nucleus of U-232 itself.

4. Estimation of the potentialities of EFR long-lived fission products transmutation

Let us assume that it is possible to create EFR blanket-target on cesium (for example, Cs-137) and zirconium (for example, Zr-93) basis with volume material fraction ratio

$$\delta_{Cs} / \delta_{Zr} = 4/1.$$

This blanket-target can be cooled with cesium or gas. Then in such a target approximately 20 neutrons are generated per one proton with 1 GeV energy. For neutron beams with parameters of $i=0.3$ A, $E_p=1$ GeV flux of $3.7 \cdot 10$ n/s will be generated in the target.

Let us consider possible transmutation capacities of long-lived fission products (LLFP) accumulated in substantial quantities in thermal reactors. LLFP can be located in the blanket on the assumption that all neutrons will be absorbed by one of the LLFP in question. Annual LLFP production of RBMK-1000 reactor is given in Table 3; as well as possible transmutation capacities of one of these nuclides in Electrofusion reactor (EFR) with preset parameters and possible RBMK-1000 - EFR reactors ratio according to transmutation of one of LLFP.

Table 3

Nuclide	Gfp (production in one RBMK-1000 reactor) kg/year eff.	Mtr (maximum trans- mutation in EFR) kg/year eff.	K=Mtr/Gfp
90-Sr	18	177	9.8
93-Zr	24	183	7.8
99-Tc	27	194	7.3

107-Pd	6.9	210	30
129- I	5.6	253	46
135-Cs	44	265	6.1
137-Cs	40	269	6.7

It sums that accept for Cs-137 it is possible to create a blanket with transmutation capacity close to that cited above. On your way to create such blankets it is necessary to solve a number of technical problems particularly on optimizing neutron absorption especially in transmuted LLFP. In case of Cs-137 such capacities seem to be hardly achievable, because the cross-section of neutron capture by Cs137 is of the same order or even lower than that of main structural materials (Zr, Al, steel), that is the probability for neutrons being absorbed by Cs-137 is approximately of the same order than that of structural materials. In other words, substantial proportion of generated neutrons will be unproductively absorbed by structural materials.

It is possible to create a target irradiated by protons on the basis of lead and zirconium (or aluminum). Neutron yield in such a target is approximately by 30 % higher, than in above-described target. Transmutation capacities and proportion ratio can be by 30 % higher, accordingly.

5. Basic problems

5.1. From the point of view of maximum neutron yield in EFR a target of uranium (thorium) should be used. The

arrangement of heat removal is the most complicated problem. The coolant decreases neutron yield by 10-20 %. 80 % of beam power is released for ~ 2 neutron paths (+50 cm) under strong exponential irregularity. The following decisions are possible: beam defocusing, profiled target, jet (dust-gaseous) target.

5.2. To increase neutron yield it is necessary to deepen beam insertion into the target.

5.3. Beam insertion into reactor volume is a substantial problem ("window problem") - cooling, vacuum, radiation resistance,

5.4. Problem of runaway - increase of the fissible nuclides content over dangerous values - refueling management, etc.

5.5. Refinement of neutron yield parameters and power density is necessary to create targets of different volumes and compositions; it is also necessary to coordinate calculation methods and data. It is expedient to carry out experiments on large multiplying targets.

Fig.1. Neutron spectrum generated in a large uranium target by proton of 1 GeV energy capacity (without fission in energy range lower than 10.5 MeV)

Fig.2. Power distribution generated by electrofusion neutrons. Designed by V. N. Sosnin (OB of MPh EI, town Obninsk) (Moscow Physical Engineering Institute)

N - БНАБ energy group

Fig. 3. Basic parameters versus irradiation time. Version I-A.

Fig. 4. Blanket basic parameters versus irradiation time. Zone of generation 180x240 cm (Version I-A)

Fig. 5. Processes rate, fission thermal power and abundant plutonium plotted against irradiation time. (Version 1-C)

Fig. 6. Blanket basic parameters changes under irradiation. (Version 2-A)

Fig. 7. Basic parameters change under blanket-target irradiation. (Version 2-B)

Fig. 8. Blanket basic characteristics change under irradiation. (Version 3-A)

Fig. 9. Power density distribution as to thickness of the blanket

Fig. 10. Z_{max} - maximum length of the zone of neutron uniform generation and distribution of volumetric material ratio Y_0 under different in metallic uranium targets

Fig. 11. E. F. neutron generation density versus the depth

of proton beam deepening into the target with uranium alternating volume content

Fig.12. (n,Xn) reaction cross-section for U-238 depending on the energy of the bombarding neutron

Fig.13. Fuel nuclide build-up under irradiation. Target version a)

Fig.14. Fuel nuclide build-up under irradiation. Target version b)

Fig.15. Fuel nuclide build-up under irradiation. Target version c)

Fig.16. Plutonium isotope composition under different levels of its build-up in fuel

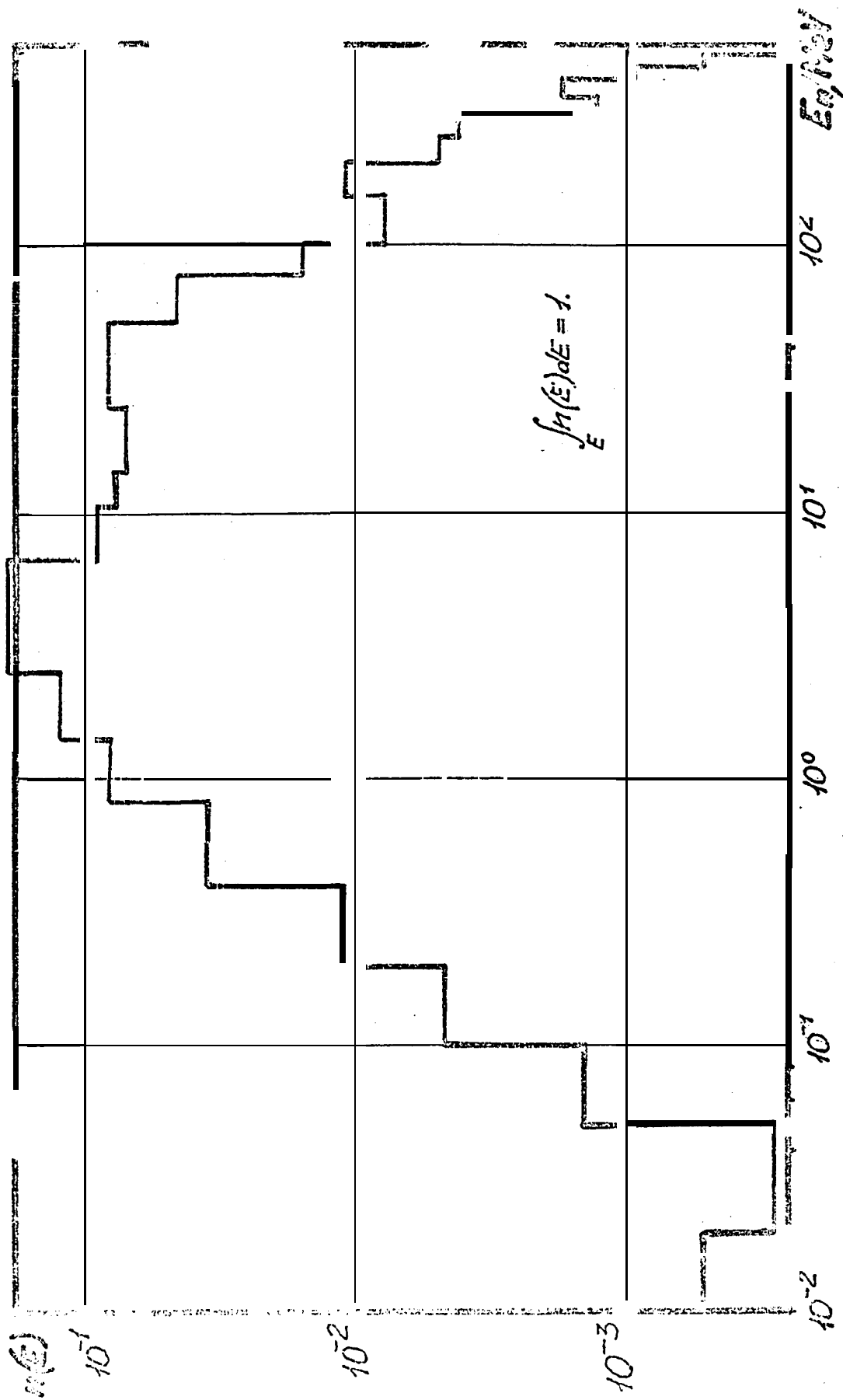


Рис. 1. Спектр нейтронов генерируемых в большой урановой мишени прогином энергией 1 ГэВ (без делений в области энергий ниже 10,5 МэВ).

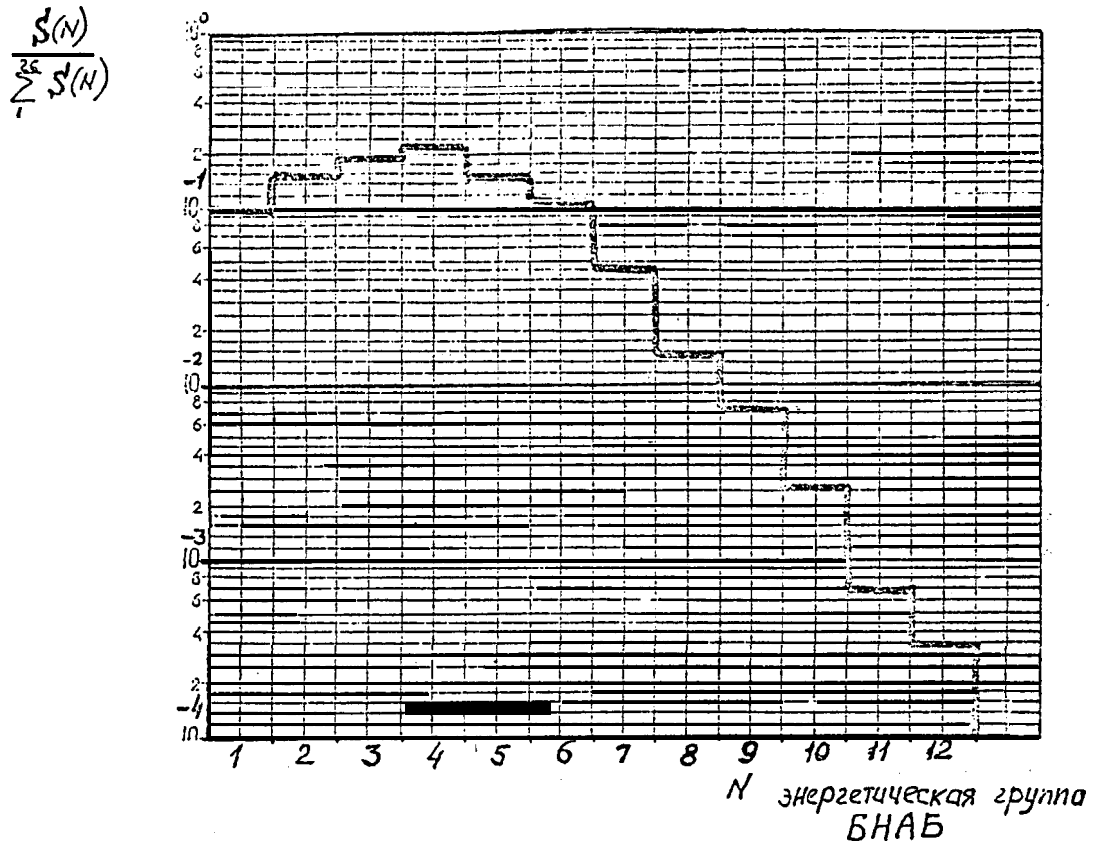


Рис. 2. Энергетическое распределение генерируемых электроядерных нейтронов.

Расчет В.Н. Соснина (ОФ МИФИ г. Обнинск).

I	-	10.5 - 6.5	МэВ
2		6.5 - 4.0	МэВ
3		4.0 - 2.5	МэВ
4		2.5 - 1.4	МэВ
5		1.4 - 0.8	МэВ
6		0.8 - 0.4	МэВ
7		0.4 - 0.2	МэВ
8		0.2 - 0.1	МэВ
9		100. - 46.5	кэВ
10		46.5 - 21.5	кэВ
11		21.5 - 10.	кэВ

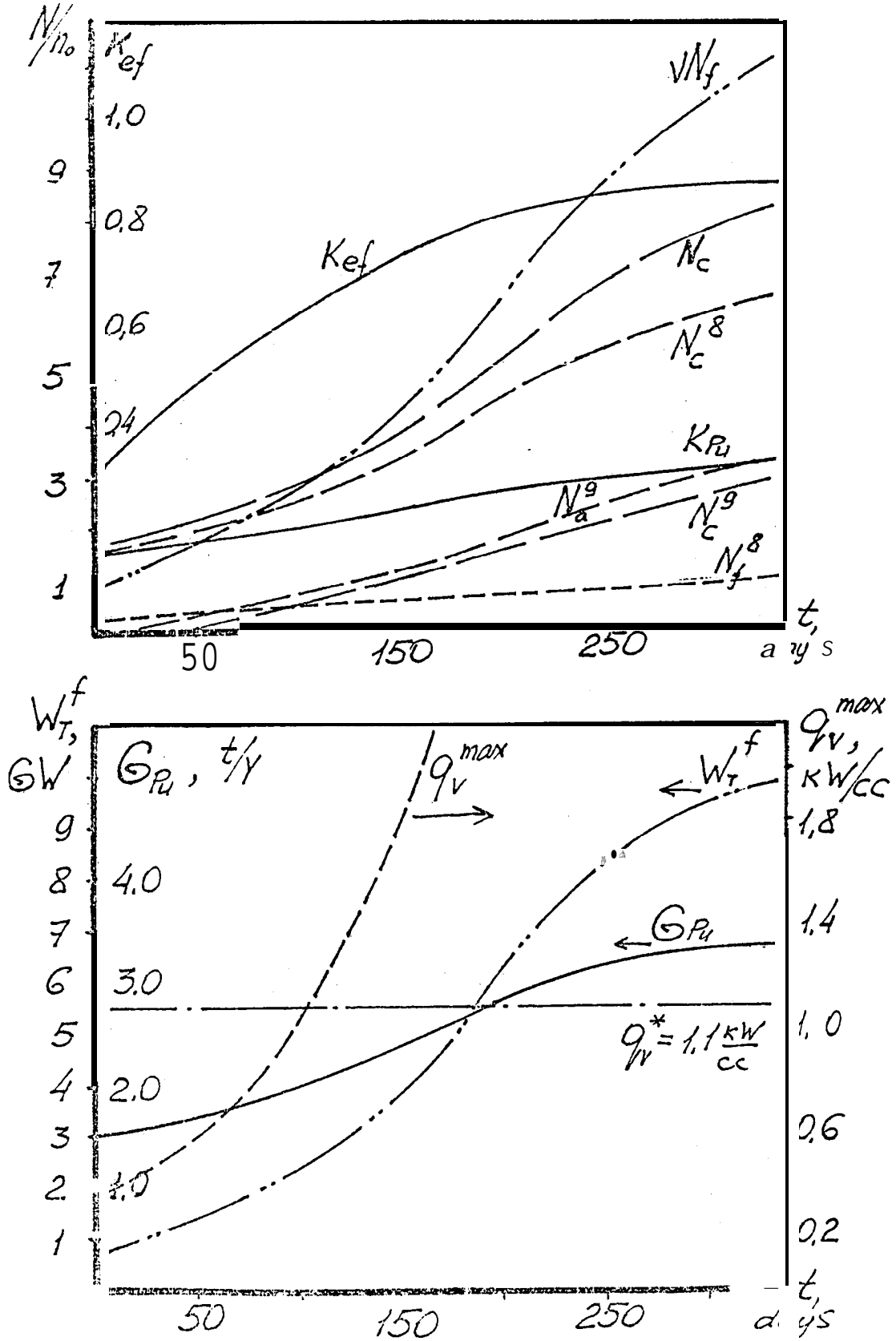


Рис. 3. Зависимость основных параметров от времени облучения. Вариант I-A.

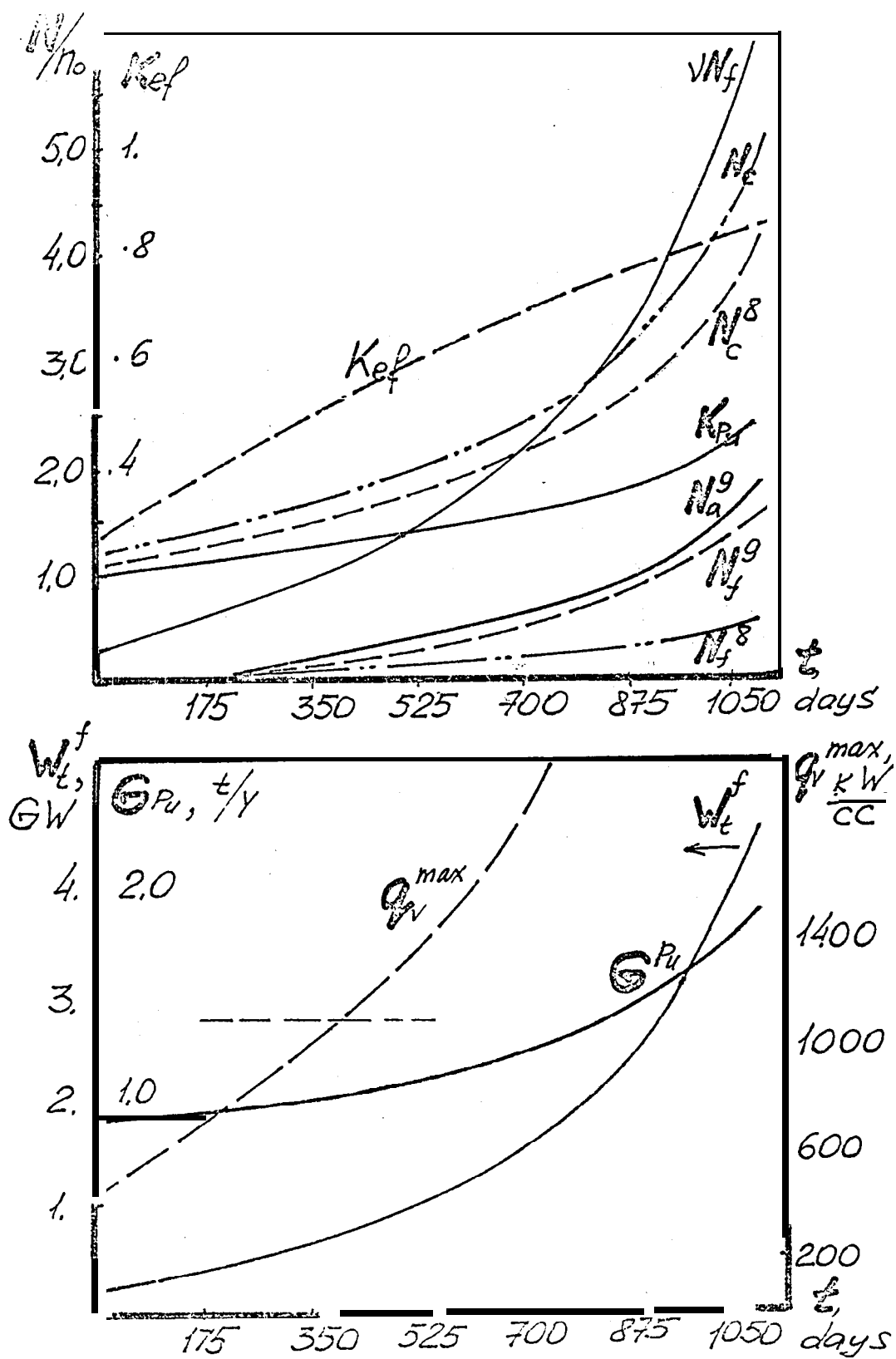


Рис. 4. Зависимость основных параметров blankets от времени облучения. Зона генерации 180 x 240 см. (вариант I-A).

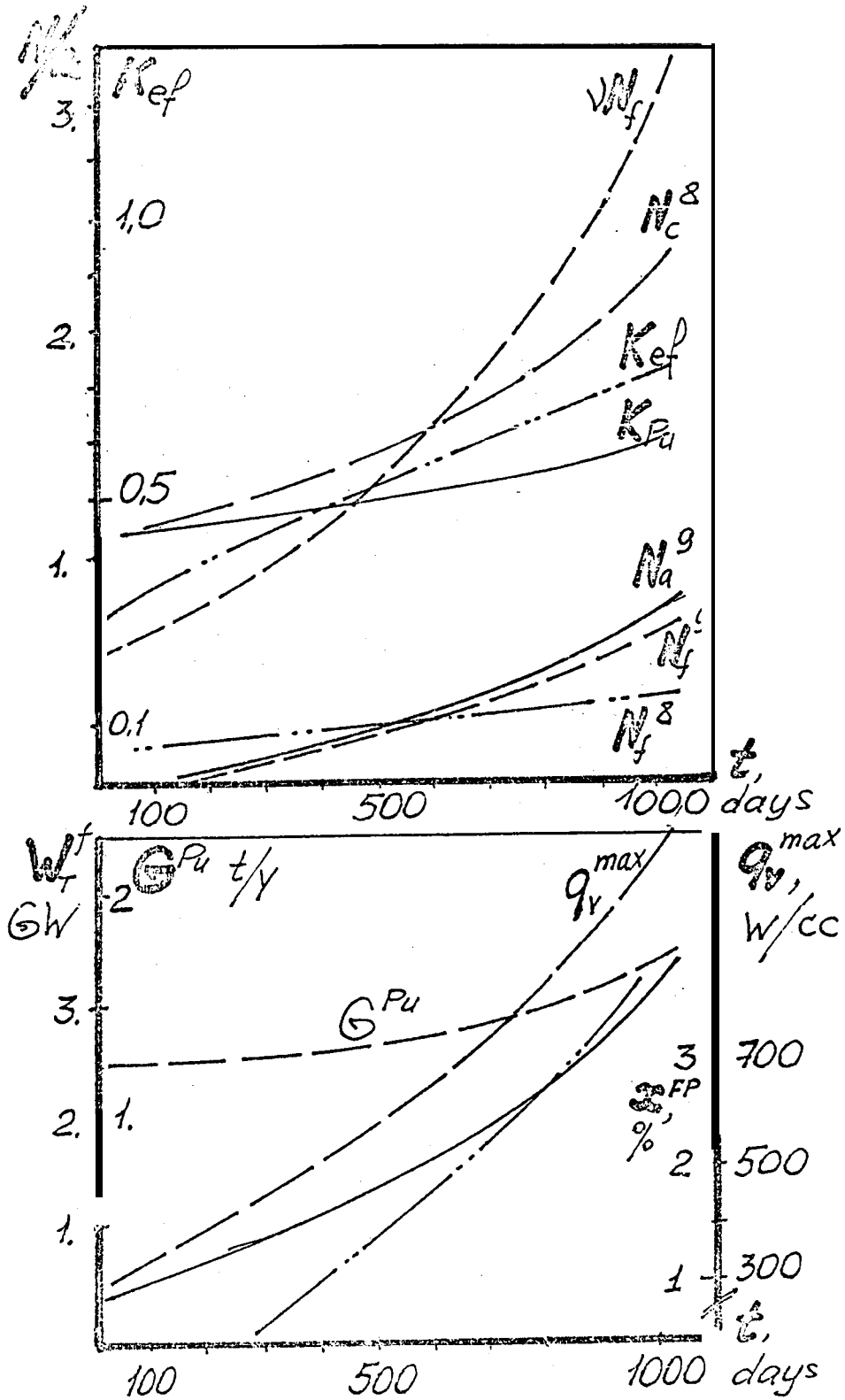


Рис. 5. Зависимость скоростей процессов, тепловой мощности деления и наработки избыточного плутония от времени облучения. Вариант 1-С.

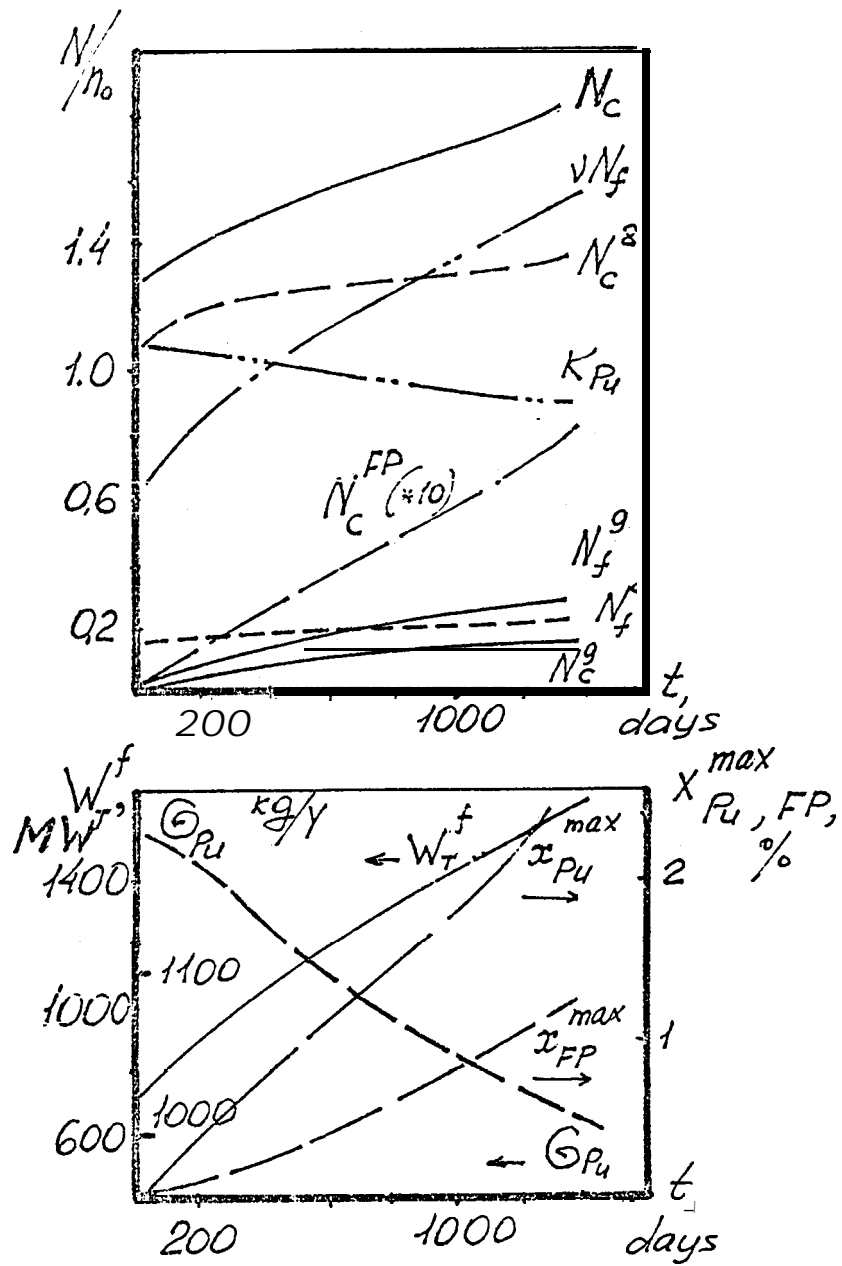


Рис. 6. Изменение основных параметров blankets при облучении (вариант 2-А).

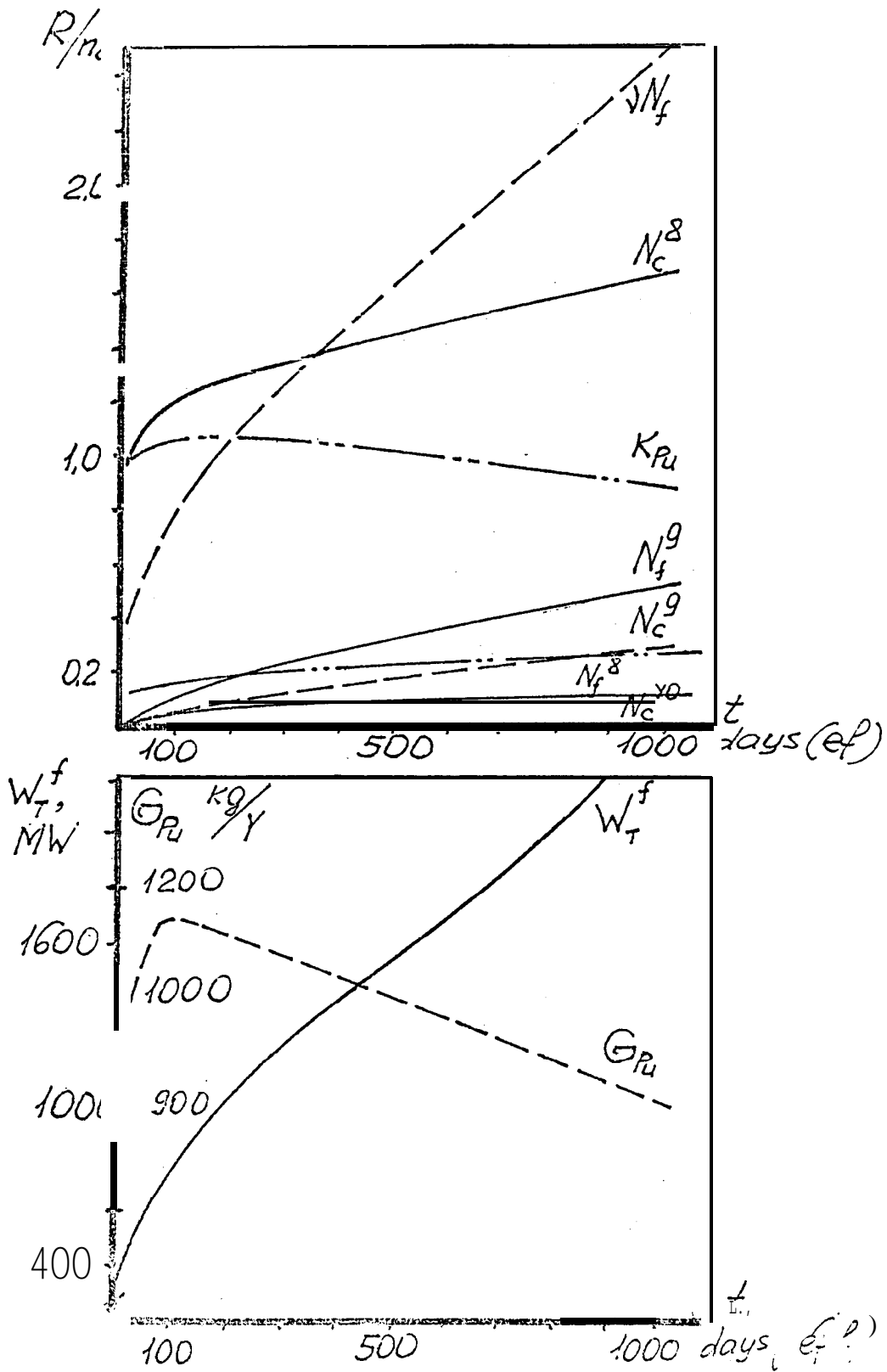


Рис. 7. Изменение основных параметров при облучении микрон-бланкета (вариант 2-В).

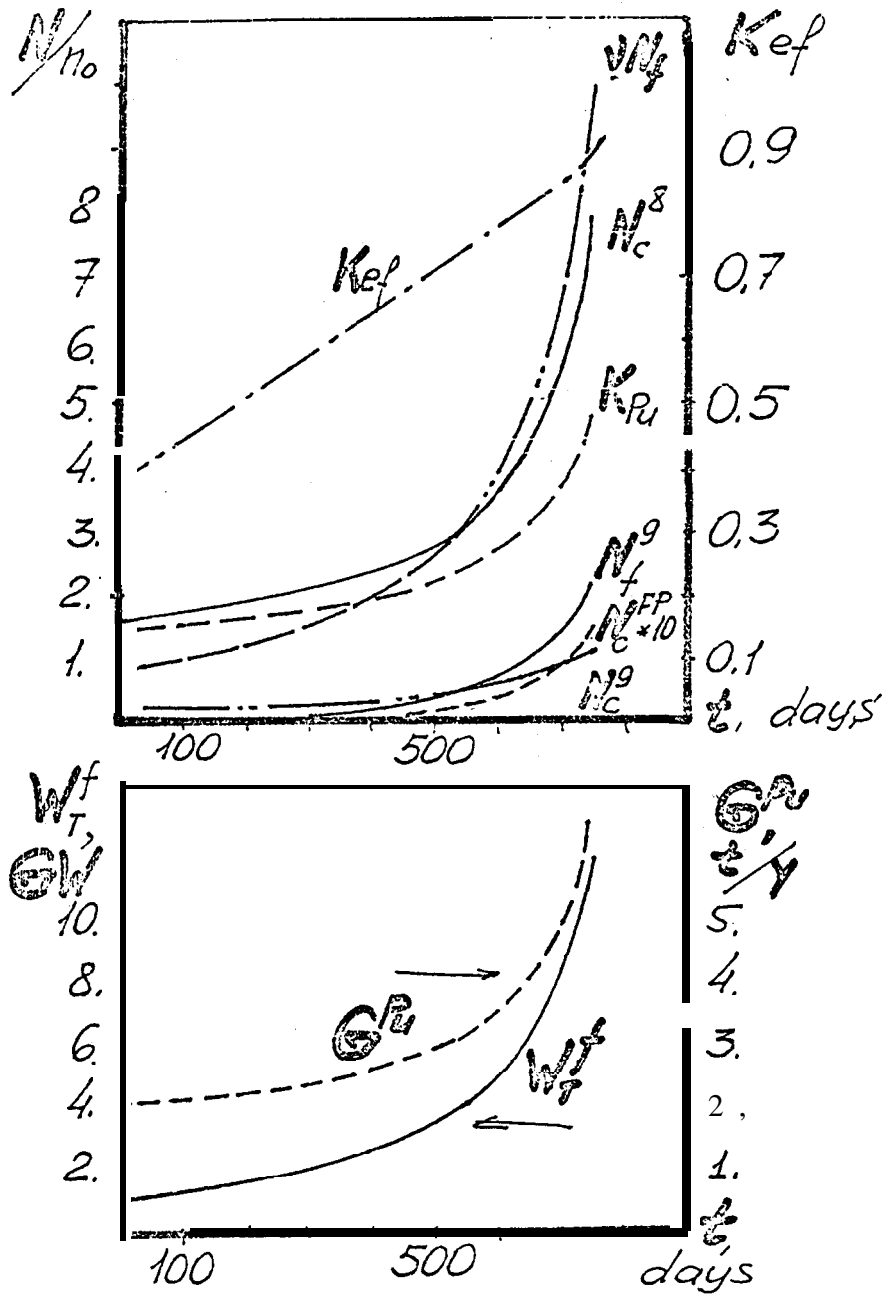


Рис. 3. Изменение основных характеристик blankets при облучении (вариант 3-А).

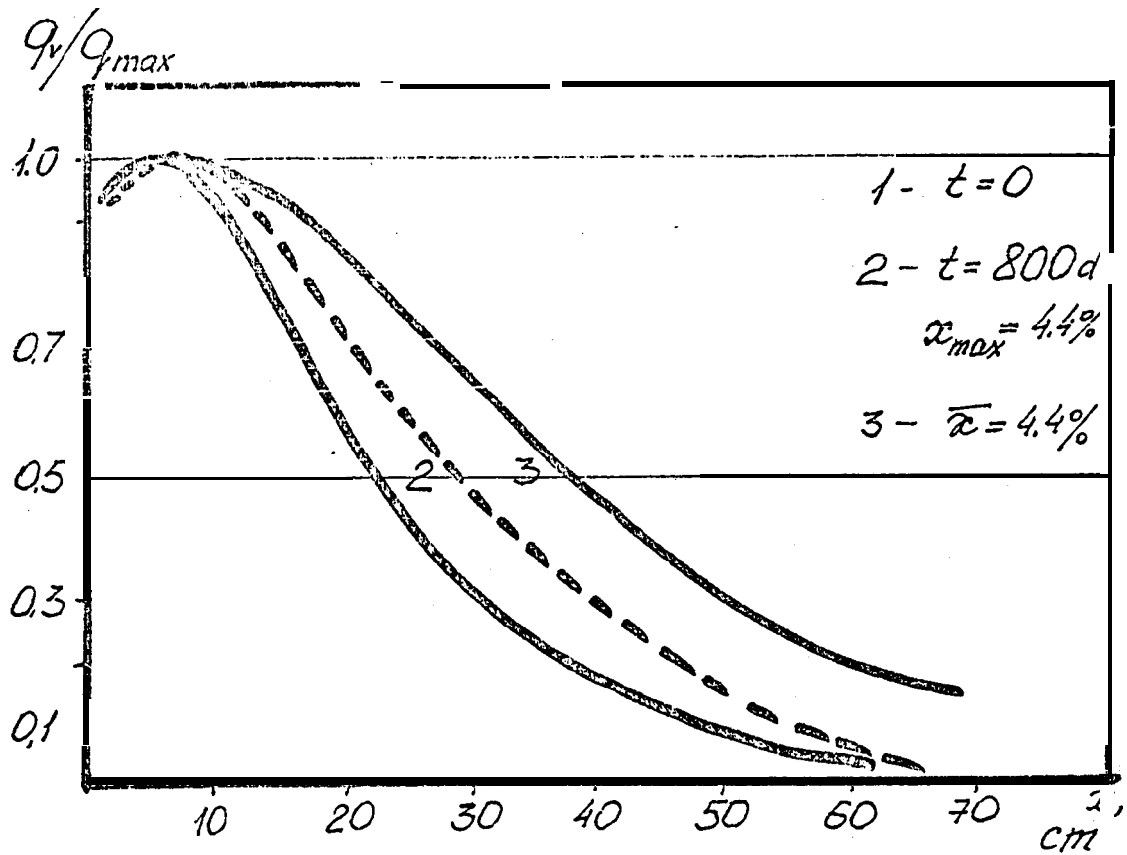


Рис. 9. Распределение энерговыделения по толщине blankets.

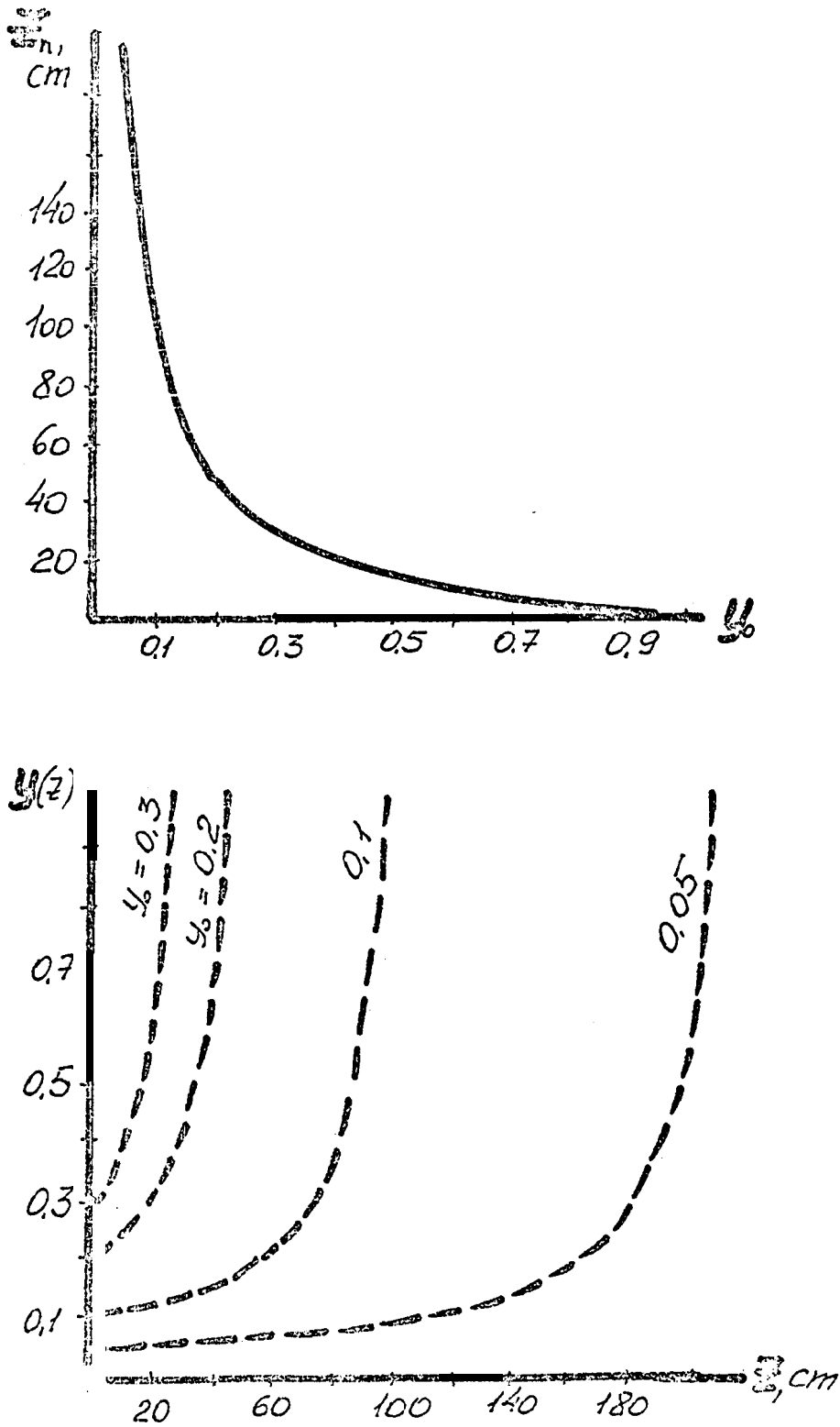


Рис. 10. Пределная длина зоны равномерной генерации нейтронов $z_{пред}$ и распределение объемной доли материала γ_0 при различных γ_0 в мишени из металлического урана.

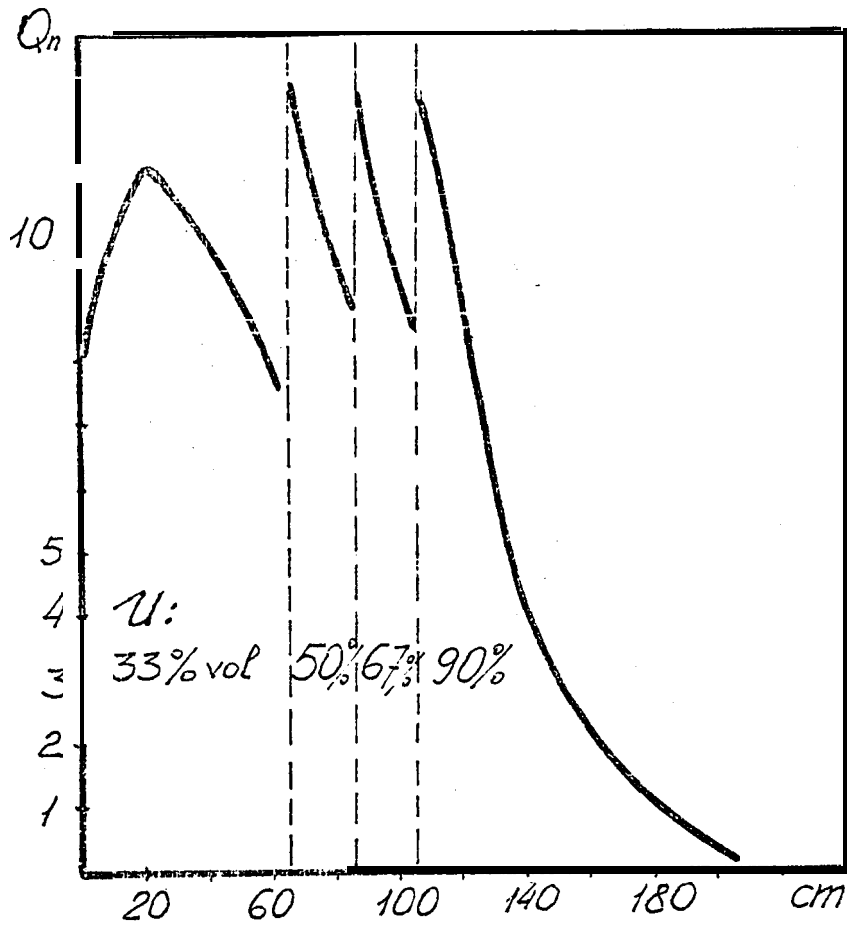


Рис. II. Зависимость плотности генерации э.я.н. от глубины погружения пучка протонов в мишени с переменным объемным содержанием урана

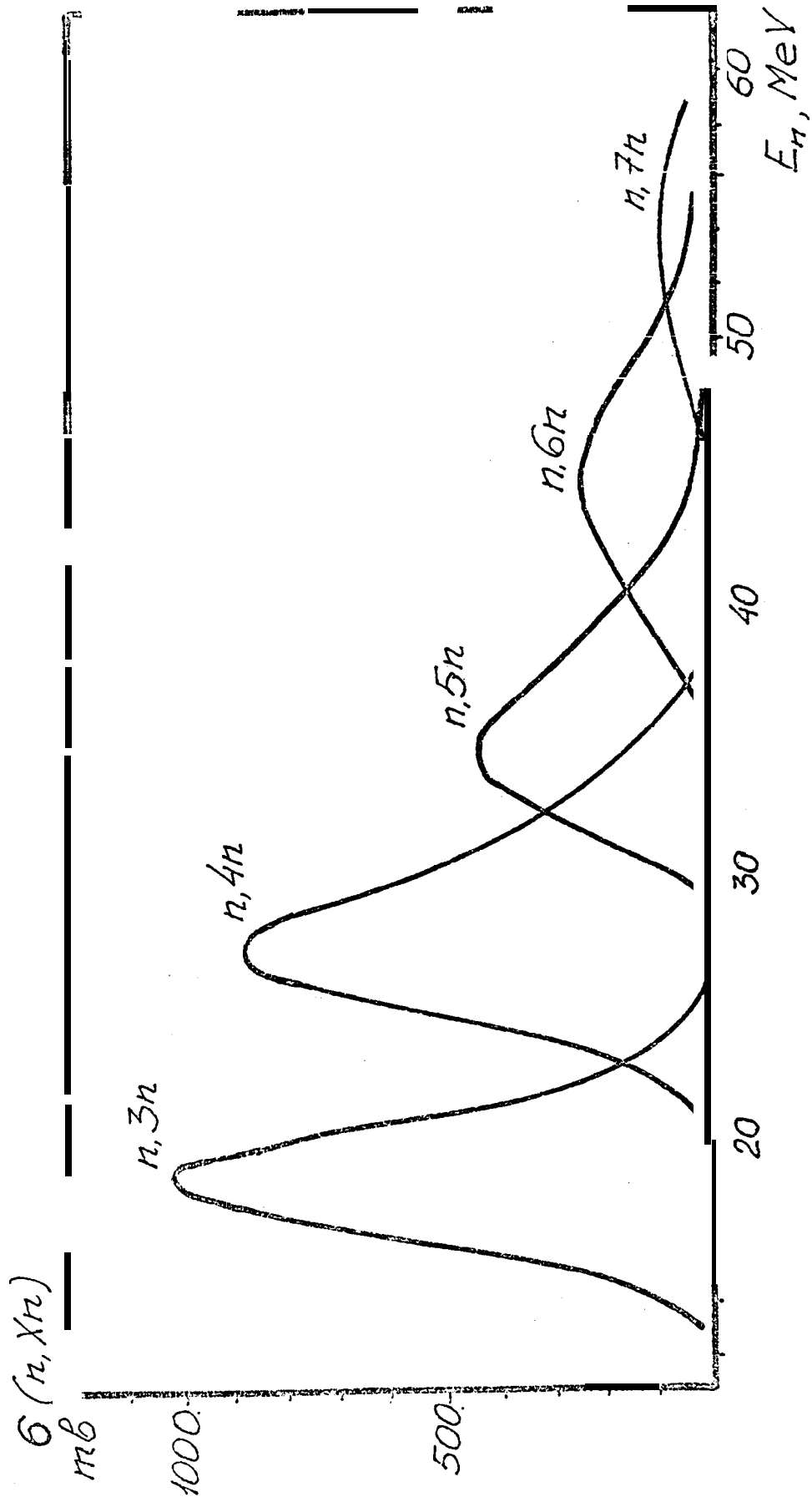


Рис. 12. Сечения реакций (n, Xn) для ^{238}U в зависимости от энергии налетающего нейтрона.

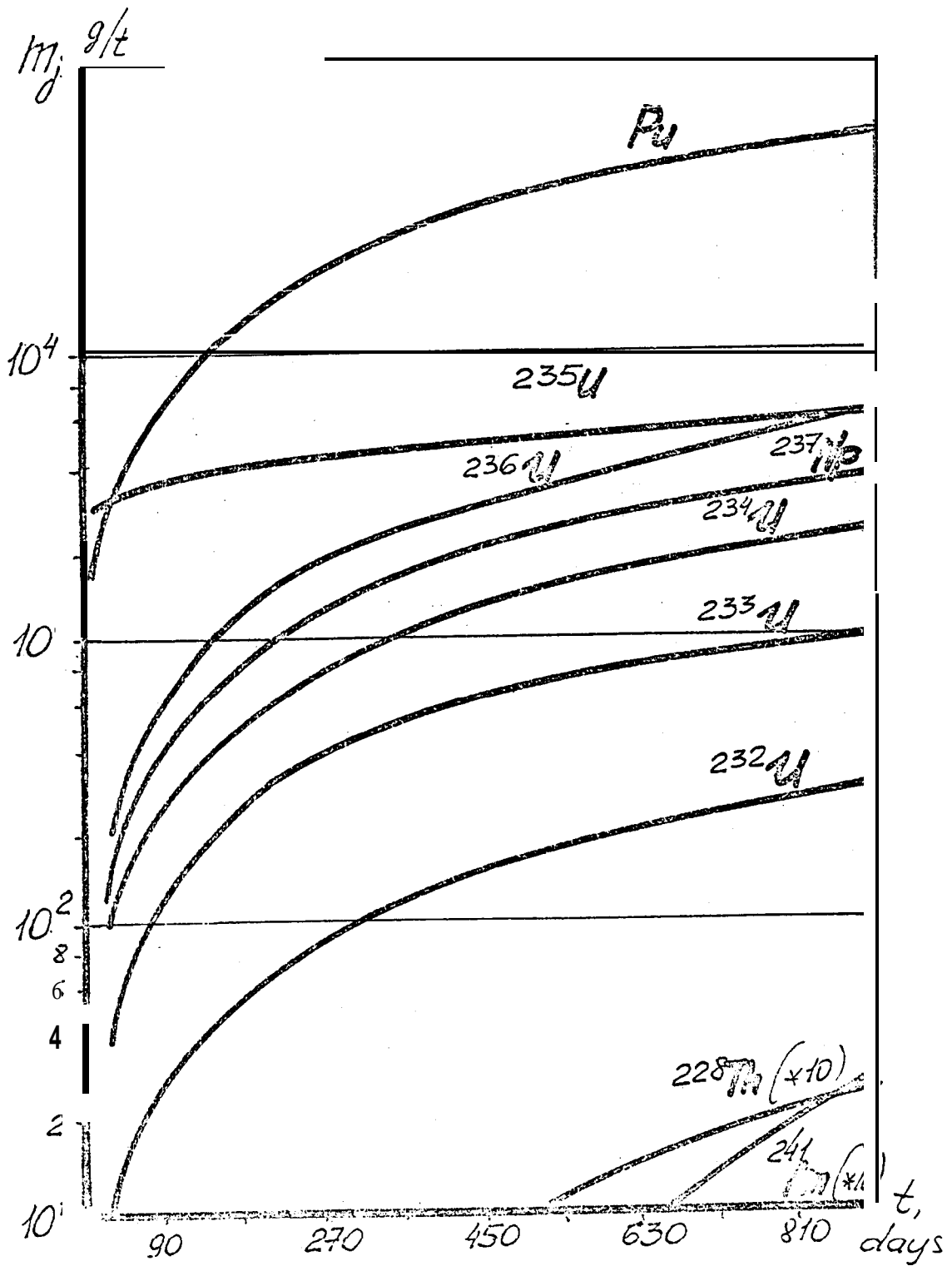


Рис. 13. Накопление нуклидов в топливе при облучении.
Вариант мишени а).

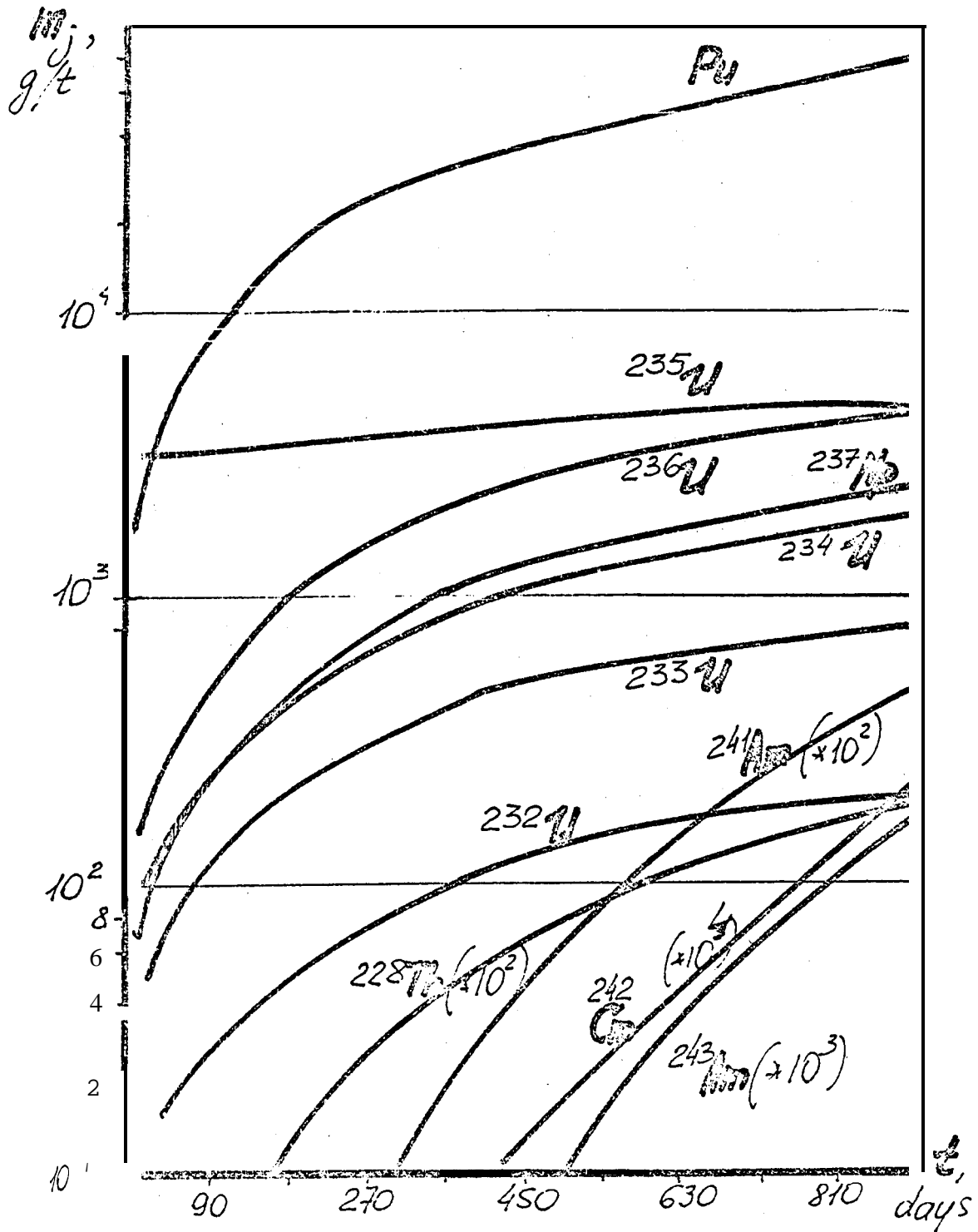


Рис. 14. Накопление нуклидов в топливе при облучении.
Вариант мишени в).

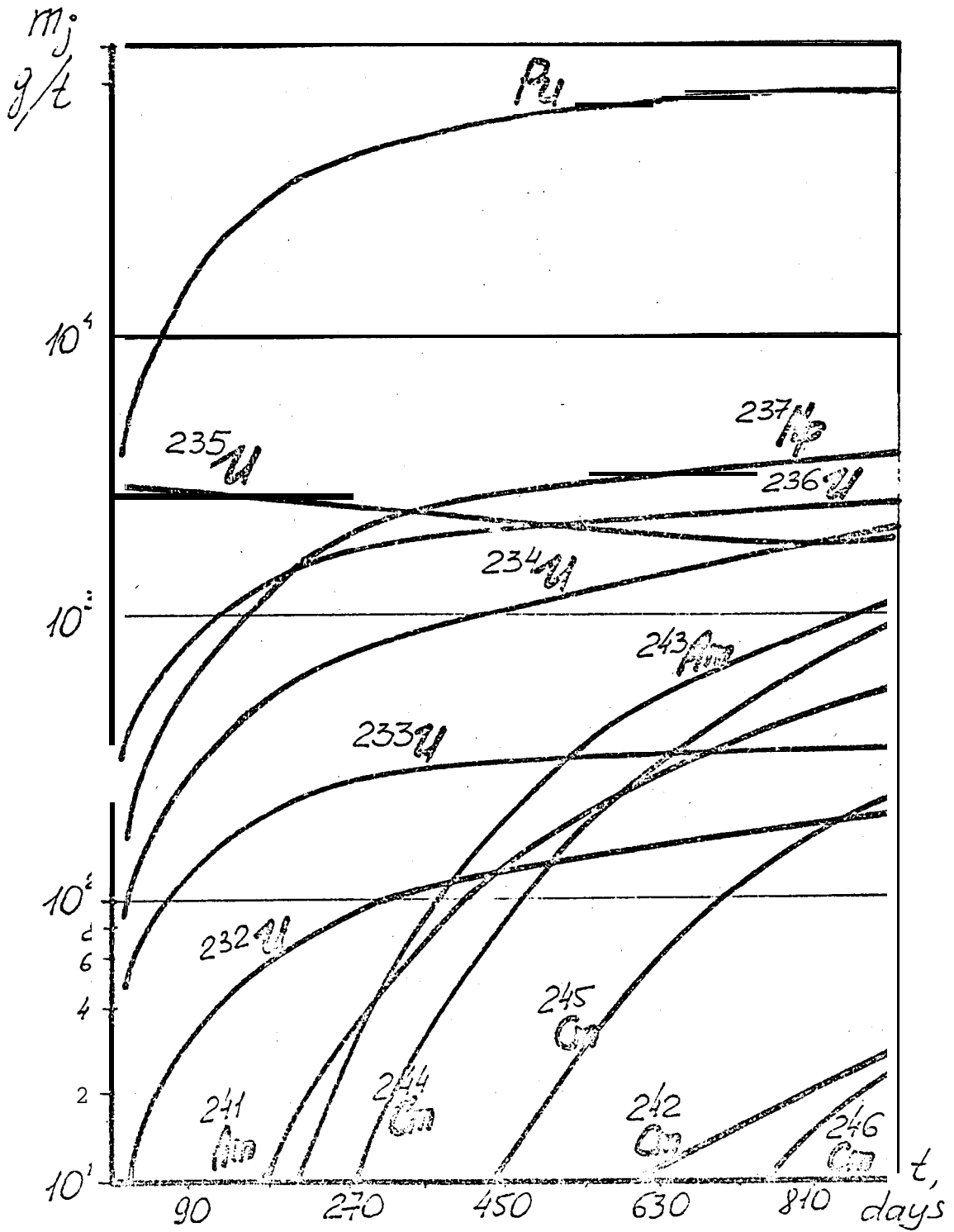


Рис. 15. Накопление нуклидов в топливе при облучении.
Вариант мишени с).

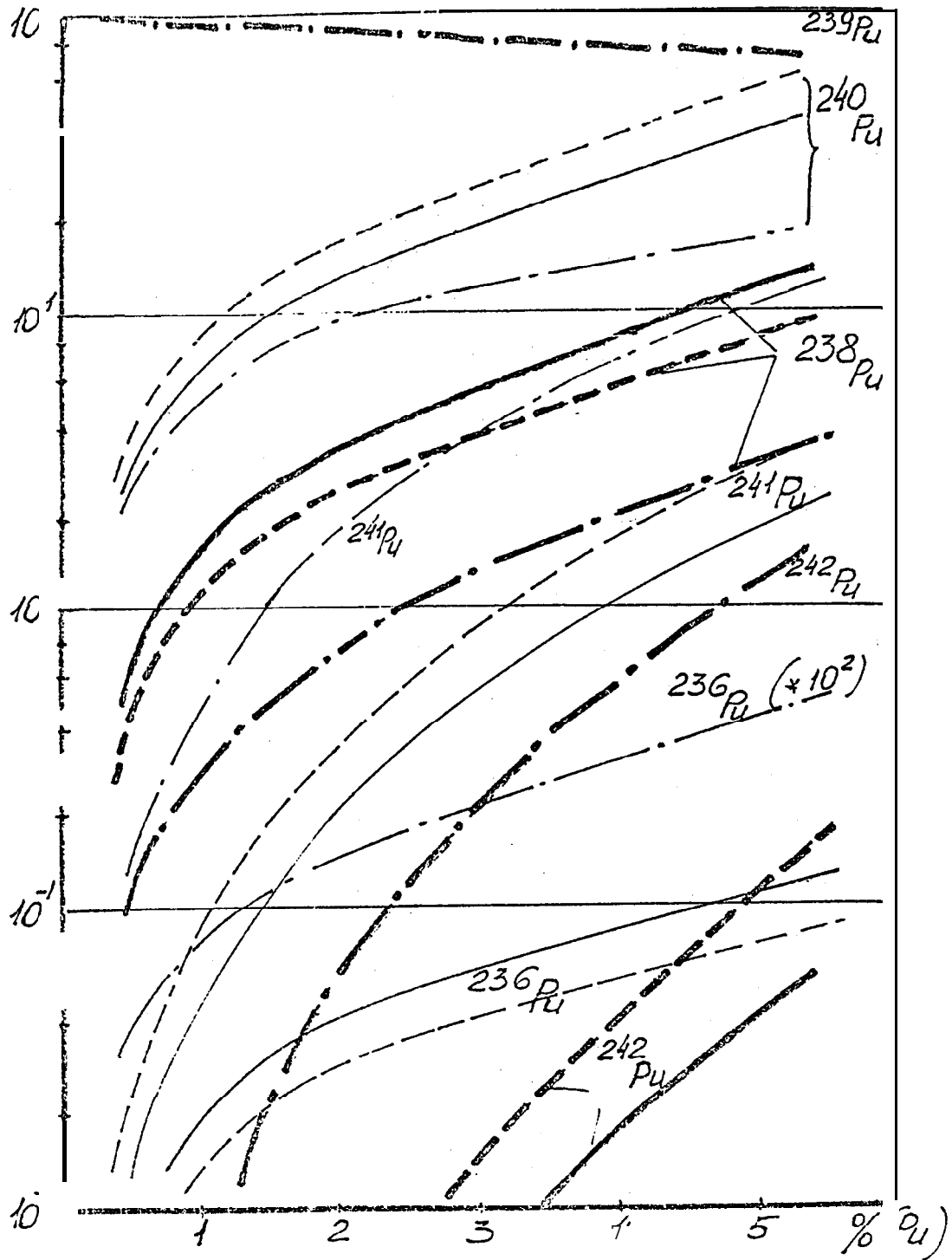
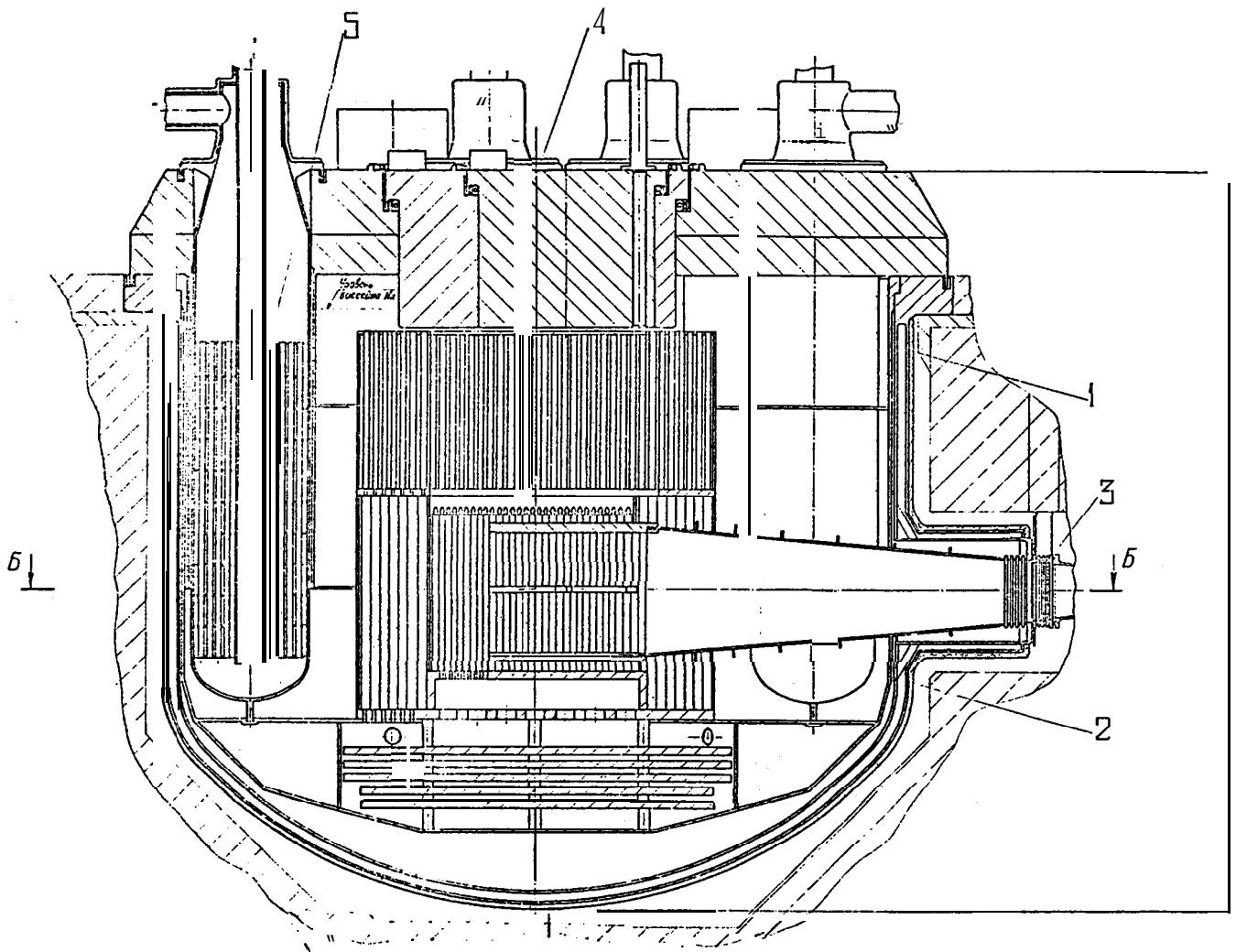
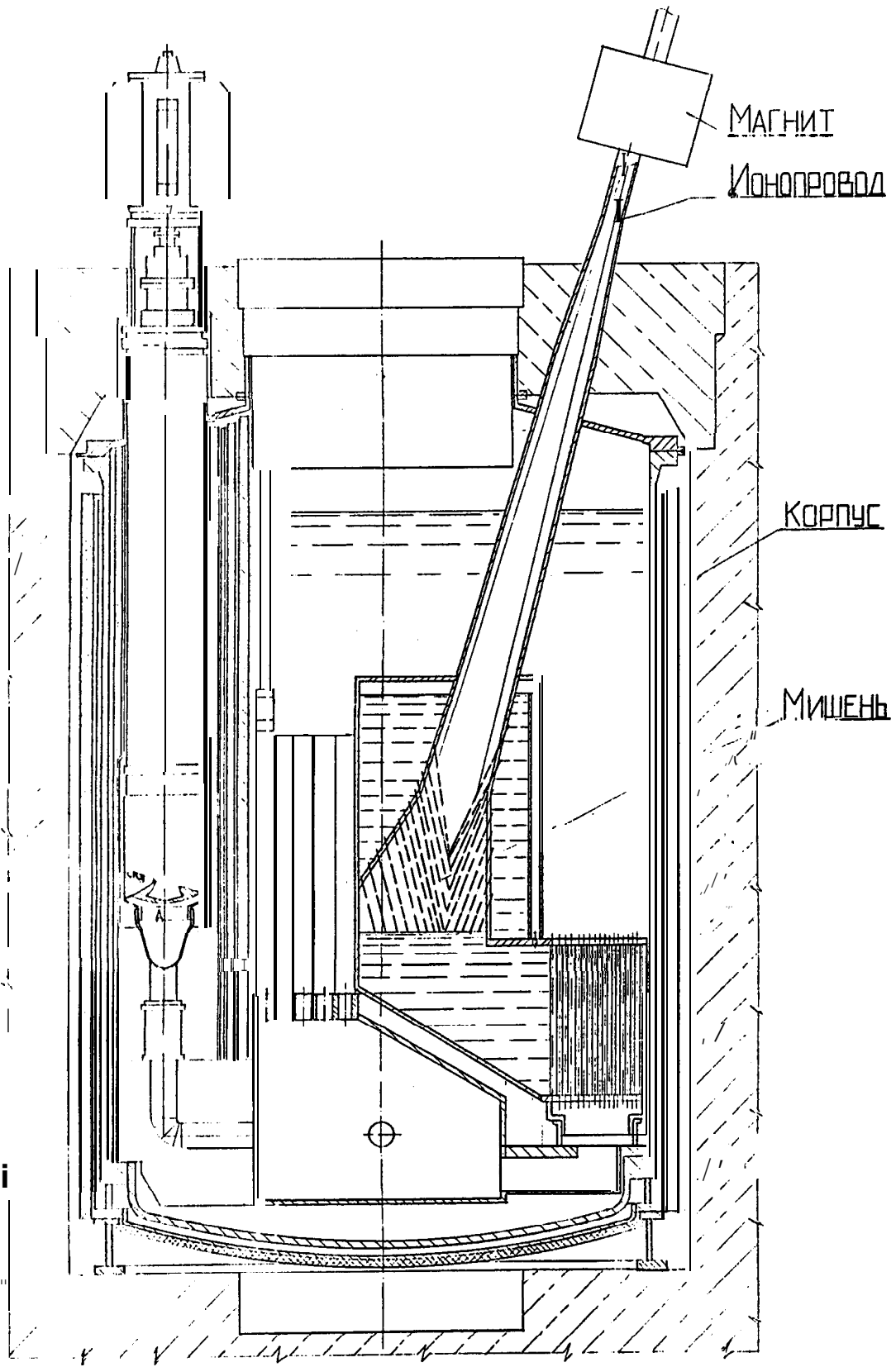


Рис. 16. Изотопный состав плутония при различных уровнях его накопления в топливе.

————— а
 - - - - - б
 - · - · - · в

A-A



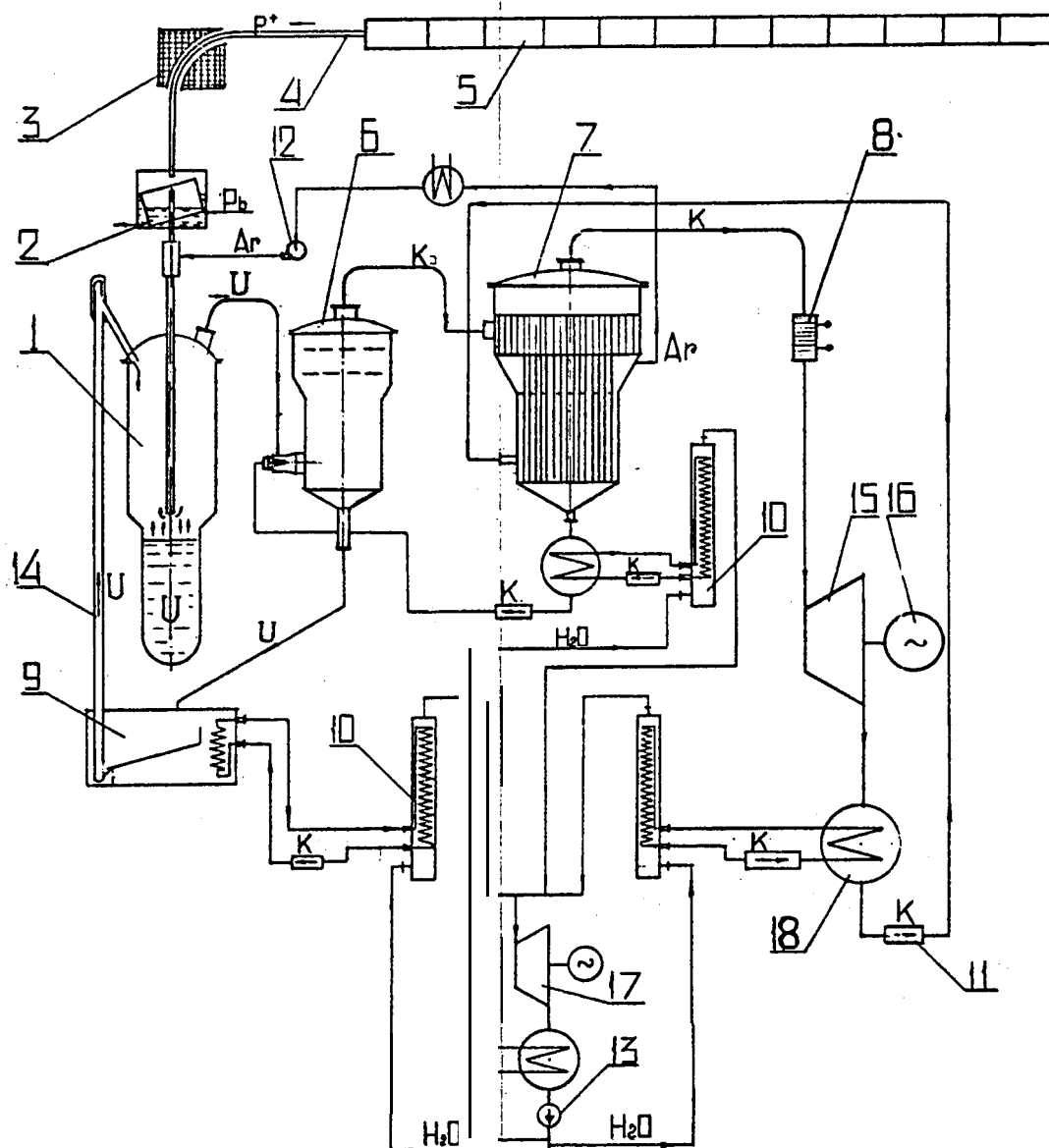


Рис СХЕМА ЭЛСИП

1-РЕАКТОР, 2-ЗАСЛОНКА, 3-МАГНИТ, 4-ИОНОПРОВОД, 5-УСКОРИТЕЛЬ,
 6-СМЕСИТЕЛЬ U-K, 7-ИСПАРИТЕЛЬ K-K, 8-МГД ГЕНЕРАТОР,
 9-ГРАНЧАЯТОР U, 10-ПАРОГЕНЕРАТОР, 11-НАСОС, 12-КОМПРЕССОР,
 13-НАСОС, 14-ЭЛЕВАТОР, 15-К-ПАРОВАЯ ТУРБИНА, 16-ГЕНЕРАТОР,
 17-ПАРОВАЯ ТУРБИНА, 18-ТЕПЛОБМЕННИК.

